

Cite this article as: Zou Ke, Deng Chunming, Zou Jianpeng, et al. Resistance Behavior to Oxidation and Molten Salt Corrosion of Supersonic Atmospheric Plasma Sprayed TiB₂-SiC Coating[J]. Rare Metal Materials and Engineering, 2021, 50(08): 2670-2677.

ARTICLE

Resistance Behavior to Oxidation and Molten Salt Corrosion of Supersonic Atmospheric Plasma Sprayed TiB₂-SiC Coating

Zou Ke^{1,2}, Deng Chunming², Zou Jianpeng¹, Liu Min², Liu Xuezhong², Zhao Ruimin³, Li Shunhua³, Zhu Renbo¹, Gao Di¹

¹ State Key Laboratory of Powder Metallurgy, Central South University, Changsha 410083, China; ² The Key Laboratory of Guangdong for Modern Surface Engineering Technology, National Engineering Laboratory for Modern Materials Surface Engineering Technology, Guangdong Institute of New Materials, Guangzhou 510650, China; ³ Yunnan Yunlv Yongxin Aluminum Company Limited, Honghe 663000, China

Abstract: The fully-coated TiB₂-SiC coating was prepared by supersonic atmospheric plasma spraying (SAPS). The oxidation performance of TiB₂-SiC coating at 400 and 800 °C was studied and the oxidation mechanism was investigated. The corrosion resistance of TiB₂-SiC coating to aluminum melting salt at 900 °C was studied, and the anti-corrosion mechanism of molten salt was discussed. The results show that the TiB₂-SiC coating prepared by SAPS has good anti-oxidation performance. The oxidation rate constant at 400 °C is $1.92 \times 10^{-3} \text{ mg}^2 \cdot \text{cm}^{-4} \cdot \text{s}^{-1}$, and that at 800 °C is $1.82 \times 10^{-4} \text{ mg}^2 \cdot \text{cm}^{-4} \cdot \text{s}^{-1}$. The TiB₂-SiC coating prepared by SAPS has good resistance to molten salt corrosion at 900 °C. TiB₂-SiC coating maintains a dense structure after molten salt corrosion, and cracking and peeling of the coating do not occur.

Key words: supersonic atmospheric plasma spraying (SAPS); TiB₂-SiC coating; oxidation resistance; resistance to molten salt corrosion

In the process of industrial aluminum electrolysis, the surface of the cathode will be electrolyzed as aluminum and sodium metal at the same time^[1,2]:



The generated Na and Al diffuse into the cathode, promoting the wettability and penetration of the molten salt electrolyte to the cathode. Under the condition of aluminum electrolysis, although the precipitation of aluminum and sodium is restricted, the precipitated sodium and aluminum melt will penetrate into the cathode material through the pores, causing the aluminum electrolytic cathode material to expand and to break, shortening the service life of the cathode material^[3-5]. TiB₂ is a high temperature ceramic material with a melting point of 2790 °C. It has good electrical conductivity, excellent wear resistance and corrosion resistance, and good

wettability with molten metal. It is an ideal inert wettability cathode material^[6]. TiB₂ material has good oxidation resistance, and the produced oxidation products of TiO₂ and B₂O₃ form a protective film on the surface of the material to inhibit the internal oxidation of the material^[7]. However, when the temperature is relatively high, due to the evaporation of B₂O₃, pores are left in the material, which increases the contact area of the material with air and deteriorates the oxidation of TiB₂. SiC has a low oxygen diffusivity, good chemical stability and high temperature oxidation resistance, which can improve the anti-oxidation performance of TiB₂^[8-10]. Moreover, the coefficient of thermal expansion of SiC is smaller, closer to that of the graphite substrate compared to TiB₂; thus SiC has a good mitigating effect on thermal stress concentration and effectively prevents the generation and diffusion of cracks.

Received date: August 15, 2020

Foundation item: Guangdong Academy of Sciences Project (2018GDASCX-0402); Yunnan Science and Technology Plan Project (2018IC080); Natural Science Foundation of Hunan Province (2018JJ2524)

Corresponding author: Deng Chunming, Ph. D., Professor, Guangdong Institute of New Materials, Guangzhou 510650, P. R. China, Tel: 0086-20-61086656, E-mail: dengchunming@gdinm.com

Copyright © 2021, Northwest Institute for Nonferrous Metal Research. Published by Science Press. All rights reserved.

At present, there are some researches on the oxidation properties of TiB₂-SiC composite ceramic materials^[11-13], most of which are sintered into bulk ceramic materials for research. There are very few reports about TiB₂-SiC composite ceramic coatings prepared by plasma spraying. Therefore, SAPS was used to prepare a fully coated TiB₂-SiC composite coating to explore its oxidation resistance and resistance to molten salt corrosion.

1 Experiment

1.1 Fully coated TiB₂-SiC coating by supersonic atmospheric plasma spraying

The TiB₂ powder and SiC powder were mixed with an appropriate amount of deionized water, followed by milling for 3 h in the planetary ball mill, and then polyvinyl alcohol was added into the slurry to continuously mill them for 3 h; finally the composite powder slurry was prepared for spray granulation. Spray granulation was made by mobile minor spray dryer produced by Gea Niro of Germany. The optimum technological parameters for spray granulation of TiB₂-SiC composite powder include 50wt% solid, 5wt% polyvinyl alcohol binder, and 10wt% SiC. The TiB₂-SiC powder after spray granulation was vacuum calcined. The organic binder was removed by holding at 300 and 500 °C for 2 h. The TiB₂-SiC powder was calcined at 1400 °C for 2 h to connect the large and small particles of TiB₂-SiC to improve the strength of TiB₂-SiC powder. With TiB₂-SiC powder after spray granulation and vacuum calcination as the sprayed powder, the surface of the graphite substrate was fully coated by the 100 HE supersonic plasma spraying system. Based on the previous research of our group, the spraying parameters shown in Table 1 were selected. Before the full coating was sprayed, the graphite substrate with the specification of $\Phi 12.7$ mm \times 20 mm was roughened, and the substrate was preheated to about 250 °C by the plasma flame flow to reduce the thermal mismatch stress between the coating and the substrate.

1.2 Anti-oxidation experiment of the TiB₂-SiC coating

The oxidation performances of TiB₂-SiC coating at 400 and 800 °C were studied. The fully coated TiB₂-SiC coating was initially weighed prior to the oxidation experiment and recorded as m_1 . The fully coated TiB₂-SiC coating was placed in a high temperature resistance furnace at corresponding temperature and oxidized for 3, 6, 9, 12 and 15 h, and then cooled to room temperature naturally. The oxidized TiB₂-SiC coating was weighed again and recorded as m_2 . Through these, the mass change rate Δw of the TiB₂-SiC coating can be calculated, and the calculation formula is as follows^[14]:

$$\Delta w = \frac{m_2 - m_1}{m_1} \quad (2)$$

1.3 Resistance to molten salt corrosion test of the TiB₂-SiC coating

The corrosion resistance of TiB₂-SiC coating at 900 °C was studied. The fully coated TiB₂-SiC coating was prepared by SAPS. The fully coated TiB₂-SiC coating was placed in a conventional electrolyte for aluminum electrolysis, and it was etched at 900 °C for 8 h to investigate its resistance to molten salt corrosion and electrolyte penetration. The electrolyte composition was 90wt% Na₃AlF₆, 5wt% CaF₂, and 5wt% Al₂O₃.

1.4 Performance characterization

The morphology of the coating was observed by nova-nano-sem-430 (with EDS analysis) field emission scanning electron microscope (SEM). The phase structure of powder and coating was analyzed by D8 advance X-ray diffractometer (Bruker, Germany). The $K\alpha$ -ray of Cu target was used as diffracted source, the scanning step was 0.02°/s, and the scanning range was 2θ from 10° to 90°. TG-DSC test was carried out on SETSYS 18/24 integrated thermal analysis system produced by Setaram Instrumentation Company in France.

2 Results and Discussion

2.1 Microstructure and phase structure of TiB₂-SiC coating oxidized at 400 °C

According to the thermogravimetric curve, the oxidation reaction has not occurred at 400 °C, and it is basically completed at 800 °C. To study the oxidation kinetics before and after oxidation reaction, 400 and 800 °C are chosen as the oxidation temperatures. The morphologies of TiB₂-SiC coating oxidized at 400 °C for 3, 9 and 15 h are shown in Fig. 1. It can be seen that after the oxidation of TiB₂-SiC coating at 400 °C for 3 h, the coating has almost no change, and the surface is smooth. There is a trace of oxidized particle distribution, and the coating structure is dense, as indicated in Fig. 1a and 1d. With the increase of oxidation time, when the TiB₂-SiC coating is oxidized at 400 °C for 9 h, a large amount of particulate matter is distributed on the surface of the coating, and the small particles are oxidized, as indicated by EDS analysis in Fig. 1g. The cross section shows a slight amount of crack generation, as shown in Fig. 1b and 1e. When the TiB₂-SiC coating is oxidized at 400 °C for 15 h, more TiO₂ oxide particles are still distributed on the surface of the coatings. The TiO₂ oxide particles on the surface of the coatings are covered by glassy materials, which is confirmed as the mixture of SiO₂ and B₂O₃ by EDS analysis (as shown in Fig. 1h). The cross-section morphology shows that the coating density increases without cracking, as shown in Fig. 1c and 1f.

The TiB₂-SiC coating is slightly oxidized at 400 °C for 3 h, and the coating morphology does not change much. With the

Table 1 Parameters of fully coated TiB₂-SiC coating prepared by SAPS

Spraying power/kW	Spraying distance/mm	Ar flow rate/ L·min ⁻¹	N ₂ flow rate/ L·min ⁻¹	H ₂ flow rate/ L·min ⁻¹	Carrier gas/L·min ⁻¹	Powder feed rate/g·min ⁻¹
95	150	40	28	34	11	14

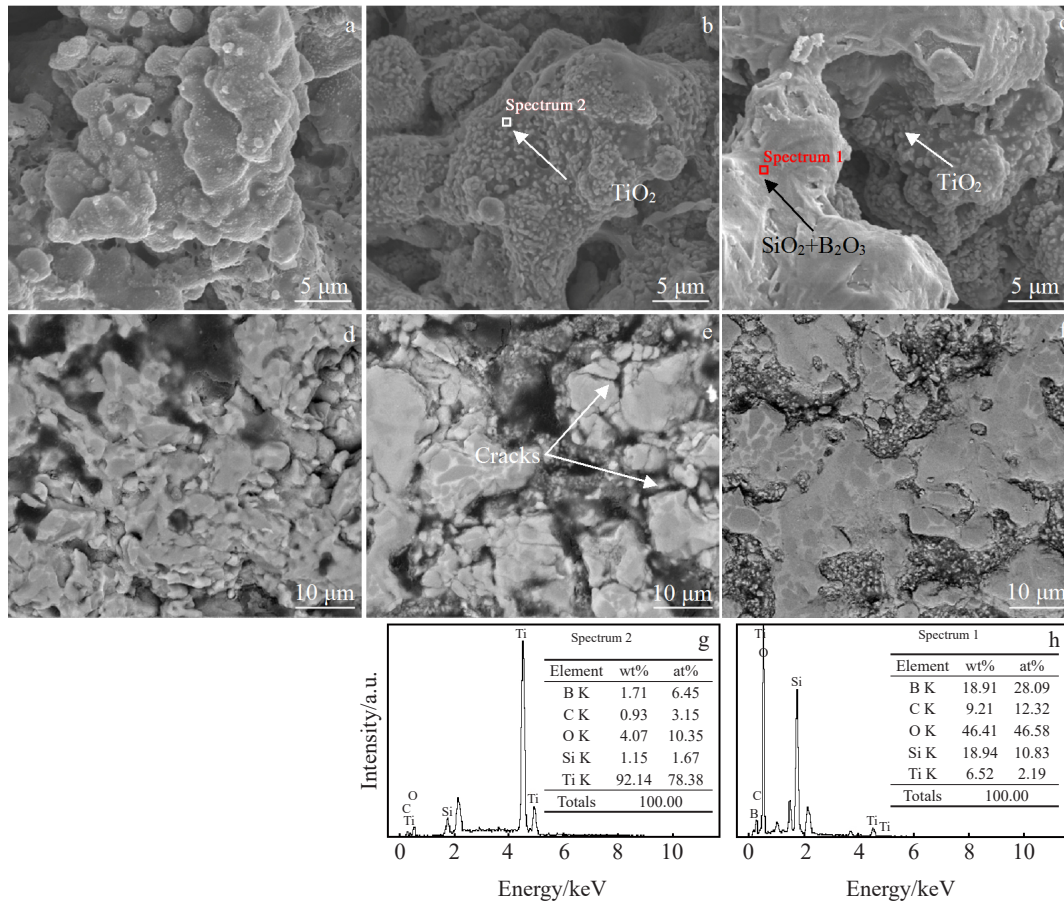


Fig.1 Surface morphologies (a-c), cross-sectional morphologies (d-f), and EDS analysis results (g, h) of $\text{TiB}_2\text{-SiC}$ coating after oxidation at $400\text{ }^\circ\text{C}$ for different time: (a, d) 3 h, (b, e, g) 9 h, and (c, f, h) 15 h

increase of oxidation time, TiO_2 is formed in the $\text{TiB}_2\text{-SiC}$ coating after oxidation at $400\text{ }^\circ\text{C}$ for 9 h, which leads to the formation of cracks in the coating. When the $\text{TiB}_2\text{-SiC}$ coating is oxidized at $400\text{ }^\circ\text{C}$ for 15 h, a small amount of glassy oxidation products of B_2O_3 and SiO_2 are formed, which seal the cracks, increase the density of the coating, and hinder the further oxidation of the coating.

XRD results of the $\text{TiB}_2\text{-SiC}$ coating oxidized at $400\text{ }^\circ\text{C}$ for 0, 3, 9, and 15 h are shown in Fig.2. The $\text{TiB}_2\text{-SiC}$ coating after SAPS is mainly composed of TiB_2 phase and SiC phase. SiC phase cannot be seen in the XRD pattern because its content is small, as shown in the curve of 0 h. When the $\text{TiB}_2\text{-SiC}$ coating is oxidized at $400\text{ }^\circ\text{C}$ for 3 h, the phase of the coating does not change significantly, but the peak of the (101) crystal plane diffraction peak of TiB_2 decreases significantly. After oxidation at $400\text{ }^\circ\text{C}$ for 9 h, new phase of TiO_2 is produced, but the crystallinity is small. When $\text{TiB}_2\text{-SiC}$ is oxidized at $400\text{ }^\circ\text{C}$ for 15 h, the diffraction peaks of TiO_2 (101) crystal plane and (211) crystal plane are enhanced, and the diffraction peak of the (111) crystal plane appears. It can be seen from the curve of 9 h that the oxidation products SiO_2 and B_2O_3 are also produced, but they cannot be detected through XRD due to their small amount, as shown in the curve of 15 h.

In summary, with the increase of oxidation time of $\text{TiB}_2\text{-SiC}$ coating at $400\text{ }^\circ\text{C}$, the $\text{TiB}_2\text{-SiC}$ coating will be slightly oxidized to form oxidized protective film of TiO_2 , B_2O_3 and SiO_2 , which can effectively isolate oxygen diffusion from the inside of the coating and retard the oxidation process of the coating, giving the coating good oxidation resistance.

2.2 Microstructure of $\text{TiB}_2\text{-SiC}$ coating oxidized at $800\text{ }^\circ\text{C}$

The microstructures of $\text{TiB}_2\text{-SiC}$ coating oxidized at $800\text{ }^\circ\text{C}$

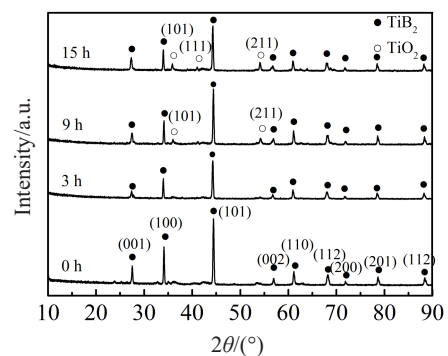


Fig.2 XRD patterns of $\text{TiB}_2\text{-SiC}$ coating oxidized at $400\text{ }^\circ\text{C}$ for 0 h, 3 h, 9 h, and 15 h

for 3, 9 and 15 h are shown in Fig.3. It can be seen that the surface of the TiB₂-SiC coating is flat and dense after the oxidation at 800 °C for 3 h, a small amount of oxides appear, and the oxidized product of TiO₂ is evenly distributed. Though a few cracks are generated in the coating, the coating is still relatively dense because of the protection of the dense glassy oxidation product SiO₂, as shown in Fig.3a and Fig.3d. When the TiB₂-SiC coating is oxidized at 800 °C for 9 h, there is a large amount of sheet-like products stack on the surface of the coating, which is analyzed by EDS as an oxidation product of B₂O₃ (as shown in Fig.3g). Part of the coating surface shows granular morphology, wrapped by glassy SiO₂. The coating still has a few cracks and holes, as shown in Fig.3b and 3e. After the TiB₂-SiC coating is oxidized at 800 °C for 15 h, the sheet-like products disappear, and the spinous oxidation product B₂O₃ is produced. The granular product TiO₂ is evenly distributed on the surface of the coating, and the coating has a large number of pores and cracks, as shown in Fig.3c and 3f.

TiB₂-SiC coating oxidizes to form TiO₂, B₂O₃ and SiO₂ at 800 °C. Thermal residual stress is generated during the oxidation process, and the glassy SiO₂ seals the cracks and holes, which reduces further oxidation of the coating. As the oxidation continues, B₂O₃ and SiO₂ are insufficient to fill the cracks and pores generated by oxidation, which increases the contact area between oxygen and TiB₂-SiC coating and reduces the oxidation resistance of the coating.

Fig.4 is the XRD results of the TiB₂-SiC coating oxidized at 800 °C for 0, 3, 9, and 15 h. When the TiB₂-SiC coating is oxidized at 800 °C for 3 h, the diffraction peaks and peaks of the TiB₂ (101) crystal plane and the (100) crystal plane significantly decrease, and the oxidized product TiO₂ forms. After oxidation at 800 °C for 9 h, the diffraction peak of TiB₂ continuously decreases, and the diffraction peaks of (112), (200), (201) and (112) planes of TiB₂ disappear. At the same time,

many diffraction peaks of TiO₂ appear according to the curve of 9 h. At 3 h, the formation of B₂O₃ phase can be deduced, but it cannot be detected at 9 h because B₂O₃ is amorphous. When the TiB₂-SiC coating is oxidized at 800 °C for 15 h, the oxidation phase of the TiB₂-SiC coating tends to be stable, and does not change much compared with that at 9 h.

In summary, it can be seen that the TiB₂-SiC coating is firstly oxidized at 800 °C to form a granular TiO₂ phase, and the oxygen diffusion rate of SiC is low, which alleviates the oxidation process of TiB₂-SiC coating. As the oxidation proceeds, a flaky B₂O₃ phase and a glassy SiO₂ phase are formed, which seal the cracks and pores generated by the oxidation, thereby effectively alleviating the further diffusion of oxygen into the interior of the coating. However, with the prolongation of oxidation time, the amount of B₂O₃ and SiO₂ are not enough to fill the cracks and pores generated by oxidation; thus the oxidation of TiB₂-SiC coating is accelerated.

2.3 Oxidation kinetics curve of TiB₂-SiC coating

The oxidation kinetics curve of TiB₂-SiC coating at 400 and 800 °C for 15 h is shown in Fig.5. It can be seen from Fig.5 that the TiB₂-SiC coating has a uniform oxidation mass gain trend at different temperatures, which is consistent with the parabolic law. When the TiB₂-SiC coating is oxidized at 400 °C, the mass gain rate is faster in the initial stage. As the oxidation time increases, the growth rate gradually becomes gentle and enters into the steady state. When the TiB₂-SiC coating is oxidized at 800 °C, the oxidation rate is fast with uniform acceleration of mass gain in the initial stage. As the oxidation goes on, the surface of the coating is covered by the oxidized protective films TiO₂, B₂O₃ and SiO₂, and the oxidation rate is gradually reduced.

The oxidation mass gain curve of the TiB₂-SiC coating conforms to the parabolic equation, i.e., it satisfies $y^2=kx$. The oxidation kinetic curves of the TiB₂-SiC coating are fitted to

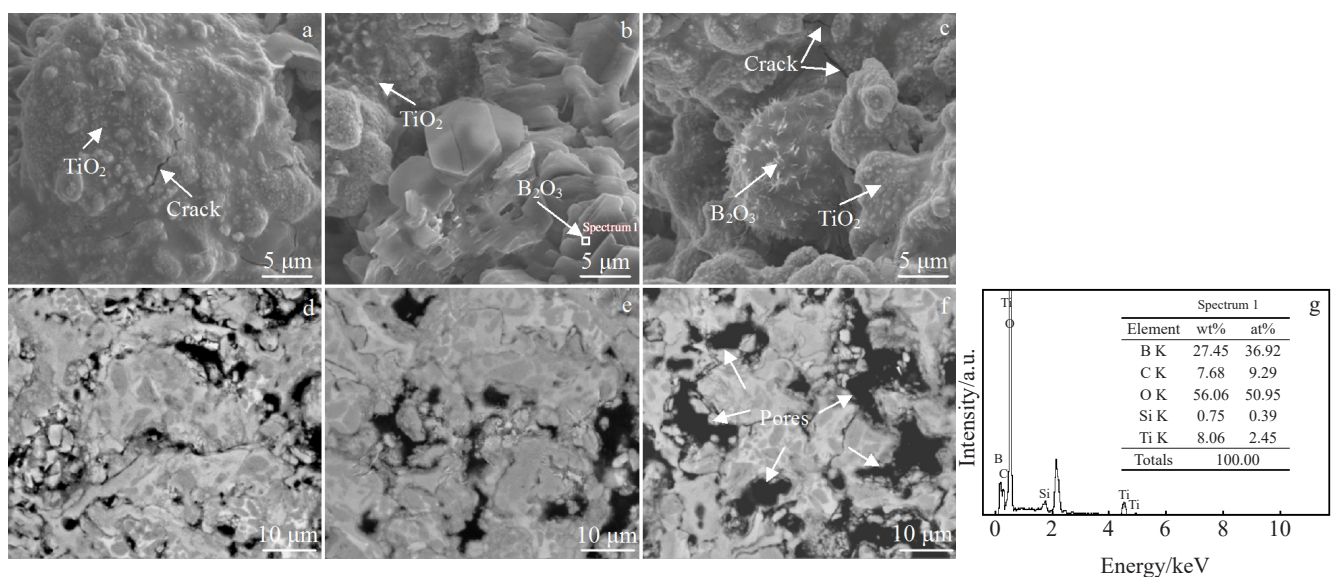


Fig.3 Surface morphologies (a~c), cross-sectional morphologies (d~f) and EDS results (g) of TiB₂-SiC coating after oxidation at 800 °C for different time: (a, d) 3 h, (b, e, g) 9 h, (c, f) 15 h

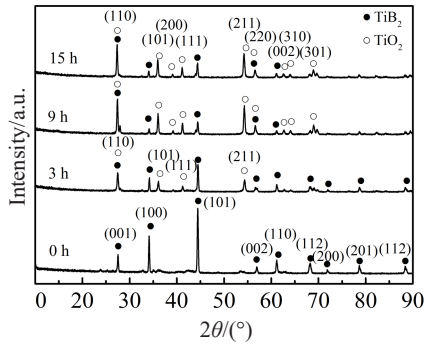


Fig.4 XRD patterns of TiB_2 -SiC coating oxidized at $800\text{ }^\circ\text{C}$ for 0 h, 3 h, 9 h, 15 h

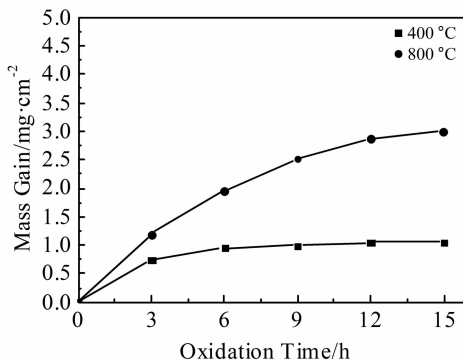


Fig.5 Oxidation kinetics curves of TiB_2 -SiC coating at 400 and $800\text{ }^\circ\text{C}$ (b)

determine the oxidation rate constants of the TiB_2 -SiC coating at 400 and $800\text{ }^\circ\text{C}$. The oxidation rate constant k_1 at $400\text{ }^\circ\text{C}$ and k_2 at $800\text{ }^\circ\text{C}$ of TiB_2 -SiC coating are 1.92×10^{-5} and $1.82 \times 10^{-4}\text{ mg}^2 \cdot \text{cm}^{-4} \cdot \text{s}^{-1}$, respectively. The oxidation rate of the TiB_2 -SiC coating at $800\text{ }^\circ\text{C}$ is one order of magnitude higher than the one at $400\text{ }^\circ\text{C}$, indicating that the higher the temperature, the faster the oxidation rate of the TiB_2 -SiC coating.

2.4 Anti-oxidation mechanism of TiB_2 -SiC coating

To further illustrate the oxidation resistance mechanism of TiB_2 -SiC coating, the thermogravimetric weight of TiB_2 and TiB_2 -SiC coating from room temperature to $1400\text{ }^\circ\text{C}$ was analyzed. Fig.6 shows the TG-DSC curves of TiB_2 and TiB_2 -SiC. It can be seen that the oxidation trends of TiB_2 and TiB_2 -SiC are basically the same.

The DSC curve in Fig.6a shows that two endothermic peaks appear at 501.2 and $717.6\text{ }^\circ\text{C}$ for pure TiB_2 , which is caused by the reaction of TiB_2 with O_2 in the air to form TiO_2 and B_2O_3 . The TG curve indicates that TiB_2 has two distinct mass gain steps in the oxidation process, corresponding to the two endothermic peaks in the DSC curve.

The DSC curve in Fig. 6b shows that two endothermic peaks appear at 516.6 and $663.6\text{ }^\circ\text{C}$ for TiB_2 -SiC coating, which is caused by the reaction of TiB_2 -SiC with O_2 in air to

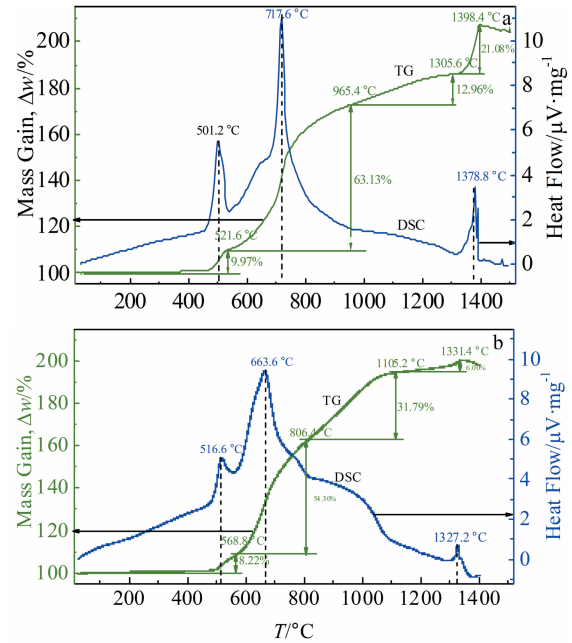


Fig.6 TG-DSC curves of TiB_2 (a) and TiB_2 -SiC (b)

form TiO_2 , B_2O_3 and SiO_2 . The TG curve indicates that TiB_2 -SiC has two distinct mass gain steps in the oxidation process, corresponding to the two endothermic peaks in the DSC curve.

According to the analysis of Fig. 6, the oxidation of TiB_2 and TiB_2 -SiC can be roughly divided into four stages, as shown in Table 2. The oxidation process of TiB_2 is as follows. (1) When the temperature is between room temperature and $521.6\text{ }^\circ\text{C}$, the mass gain rate is 9.97% . At this time, the surface of TiB_2 begins to slowly oxidize to form solid phase TiO_2 and B_2O_3 . The peak of $501.2\text{ }^\circ\text{C}$ corresponds to the melting point of B_2O_3 . With the melting of B_2O_3 , the heat is absorbed and the amount of oxidation is unchanged, so the mass gain is not high. (2) When the temperature is $521.6\text{--}964\text{ }^\circ\text{C}$, the mass gain rate is 63.13% . As the temperature increases, the oxidation process accelerates, the products TiO_2 and B_2O_3 increase continuously, and the oxidation mass gain is very large. (3) When the temperature is $964\text{--}1306\text{ }^\circ\text{C}$, the mass gain rate is 12.96% . As the temperature increases, the oxidation accelerates, but the liquid phase B_2O_3 blocks the pores and cracks, and inhibits the oxidation progress. (4) When the temperature is $1306\text{--}1389.4\text{ }^\circ\text{C}$, the mass gain rate is 21.08% . The peak value of $1378.8\text{ }^\circ\text{C}$ corresponds to the volatilization temperature of B_2O_3 , and B_2O_3 will slowly evaporate. The higher the temperature, the faster the evaporation rate, the

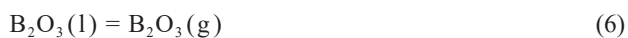
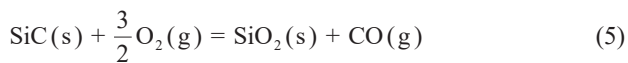
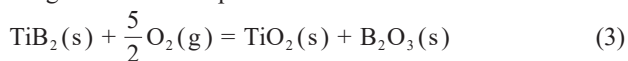
Table 2 TG-DSC analysis results of TiB_2 and TiB_2 -SiC

Stage	TiB_2		TiB_2 -SiC		
	$T/^\circ\text{C}$	$\Delta w/\%$	Stage	$T/^\circ\text{C}$	$\Delta w/\%$
1	25~521.6	9.97	1	25~568.8	8.22
2	521.6~964	63.13	2	568.8~806.4	54.30
3	964~1306	12.96	3	806.4~1082.4	31.79
4	1306~1389.4	21.08	4	1082.4~1331.4	6.00

smaller the inhibition effect of the glassy B_2O_3 as the oxygen diffusion layer, the faster the oxidation rate, and the lower the oxidation resistance.

The oxidation process of TiB_2 -SiC is as follows. (1) When the temperature is between room temperature and $568.8\text{ }^\circ\text{C}$, the mass gain rate is 8.22%. At this time, TiB_2 -SiC is slightly oxidized^[15], and solid phase TiO_2 and B_2O_3 are formed, and the mass gain is not obvious. (2) When the temperature is $568.8\sim 806.4\text{ }^\circ\text{C}$, the mass gain rate is 54.30%. Compared with pure TiB_2 , TiB_2 -SiC has a smaller absorption peak, and the mass gain rate also decreases significantly, indicating that the addition of SiC effectively inhibits the oxidation of TiB_2 . (3) When the temperature is $806.4\sim 1082.4\text{ }^\circ\text{C}$, the mass gain rate is 31.79%. As the temperature increases, the oxidation accelerates, but the liquid phases B_2O_3 and SiO_2 block the pores and cracks, and the oxidation rate is alleviated. (4) When the temperature is $1082.4\sim 1331.4\text{ }^\circ\text{C}$, the mass gain rate is 6.00%. The evaporation of B_2O_3 accelerates the oxidation and decreases the oxidation resistance, but the glassy SiO_2 slows down the oxidation process of TiB_2 -SiC. The addition of SiC improves the oxidation resistance of TiB_2 .

Combined with the previous analysis, it can be concluded that the following chemical reactions occur in the TiB_2 -SiC coating from room temperature to $1400\text{ }^\circ\text{C}$:



When the temperature is lower than $500\text{ }^\circ\text{C}$, the TiB_2 -SiC coating undergoes a slight oxidation reaction to form a solid phase oxidized protective film TiO_2 and B_2O_3 to avoid internal oxidation of the coating material. As the temperature increases, the oxidation time increases, TiB_2 -SiC coating produces dense glassy oxidation product B_2O_3 and SiO_2 , which can seal pores and cracks generated by oxidation, and effectively alleviate further oxidation of TiB_2 -SiC coating. When the temperature reaches $1082.4\text{ }^\circ\text{C}$, some liquid B_2O_3 begins to volatilize, resulting in pores in the coating, which causes a larger contact area of the TiB_2 -SiC coating with air

and accelerates the oxidation of the coating.

During the oxidation process, the oxidized product TiO_2 acts as a hard "skeleton" for the TiB_2 -SiC coating, supporting the entire coating system^[16]. The oxidized product SiO_2 has a low oxygen diffusion rate, which can effectively isolate the internal coating from contact with air and slow the oxidation rate of the TiB_2 -SiC coating. At the same time, SiO_2 behaves viscous flow property at high temperature, which can block the pores and cracks generated during the oxidation of the TiB_2 -SiC coating, and give the coating a "self-healing" ability^[17,18]. Therefore, the oxidation resistance of the TiB_2 -SiC coating can be significantly improved by adding the second phase of SiC.

2.5 Corrosion resistance of TiB_2 -SiC coating

Since $900\text{ }^\circ\text{C}$ is close to the practical application temperature, it is chosen for the molten salt corrosion resistance research for TiB_2 -SiC coating. The microscopic morphologies of the TiB_2 -SiC coating melted in aluminum solution for 8 h are shown in Fig. 7. After the TiB_2 -SiC coating prepared by SAPS is etched in the molten salt, the surface is covered with a dense glassy substance without obvious molten salt adhesion and fine cracks on the surface, as shown in Fig. 7a. This is because the TiB_2 -SiC coating prepared by SAPS is very dense, and the molten salt is difficult to adhere to the surface of the TiB_2 -SiC coating. At the same time, the cooling process of oxidized product of B_2O_3 generates thermal residual stress and causes cracks.

It can be seen from Fig. 7b that the cross section morphology of the TiB_2 -SiC coating after molten salt corrosion can be divided into four layers: a molten salt layer, an outer etching layer, an inner etching layer and a substrate layer^[19]. The molten salt layer has a clear boundary with the TiB_2 -SiC coating. The outer corrosion layer has a loose structure, and the inner corrosion layer is dense and tightly bonded to the substrate.

In order to further understand the corrosion of TiB_2 -SiC coating by aluminum electrolyte, the element distribution of TiB_2 -SiC coating after molten salt corrosion was analyzed. Fig. 8 shows the elemental distribution after salt corrosion of TiB_2 -SiC coating prepared by SAPS. It can be seen that TiB_2 -SiC coating prepared by SAPS still maintains a dense

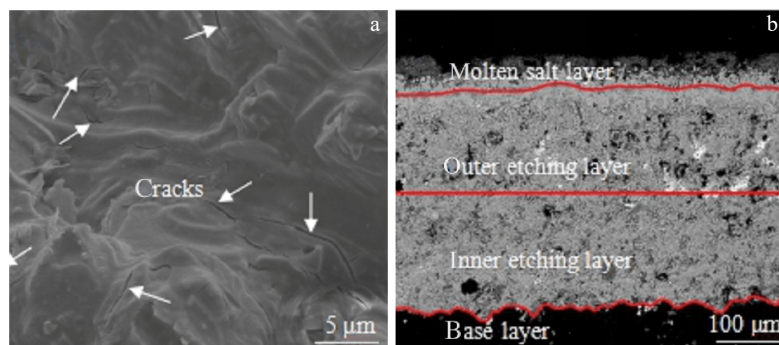


Fig.7 SEM images of surface (a) and cross sectional (b) morphologies for TiB_2 -SiC coating prepared by SAPS after molten salt corrosion

structure after corrosion, and no cracking and peeling of the coating occur. Ti and Si are uniformly distributed in the TiB_2 -SiC coating, and a slight oxidation reaction occurs. The molten salt elements such as Al and F are mainly concentrated in the molten salt layer, also distributed in the outer etching layer and the inner etching layer partially, and not diffused to the graphite matrix, as shown in Fig.8.

2.6 Corrosion resistance mechanism of TiB_2 -SiC coating

At present, there are two main viewpoints on the corrosion infiltration mechanism of aluminum electrolytic molten salt to cathode materials: one is the sodium vapor migration mechanism proposed by Dell^[20], and the other is the diffusion mechanism proposed by Li^[21]. The mechanism of sodium vapor migration is considered to be that the boiling point of sodium is lower than that of molten aluminum, and sodium insertion first occurs in the porous portion of the carbon material, so sodium migrates into the interior of the carbon material in the form of sodium vapor. The diffusion mechanism assumes that sodium is diffused into the crystal lattice and grain boundaries of the cathode material by permeation. Using molten salt electrodeposited TiB_2 coated graphite as a cathode for aluminum electrolysis, Ban^[22] found a small amount of Na in the graphite matrix. Therefore, the use of such coating as a cathode can only temporarily hinder and slow the generation and penetration of Na. In contrast, the TiB_2 -SiC coating prepared by plasma spraying is dense in

structure and can effectively resist molten salt corrosion and electrolyte penetration.

Since the temperature of the molten salt experiment is higher than the boiling point of sodium, there is also a corrosion of the TiB_2 -SiC coating by sodium vapor during the diffusion of the molten salt. The TiB_2 -SiC coating has good wettability with aluminum liquid and can form a dense aluminum liquid protective layer on the surface of TiB_2 -SiC coating. When the molten salt electrolyte penetrates into the substrate and the cathode material expands and breaks, it must pass through the aluminum liquid layer on the surface of the TiB_2 -SiC coating. As a barrier layer of the cathode, the TiB_2 -SiC coating prevents the penetration of the molten salt electrolyte into the substrate and to suppress the generation of Na. The higher the TiB_2 content in the TiB_2 -SiC coating, the better the wettability with the aluminum liquid and the stronger the cathodic protection^[23]. At this time, the electrolytes produced by the molten salt must first pass through the aluminum liquid layer, then pass through the TiB_2 -SiC coating, and finally diffuse into the graphite substrate. The aluminum liquid electrolyte needs a longer period of time to penetrate into the cathode graphite substrate with the TiB_2 -SiC coating than into the ordinary graphite substrate, so the TiB_2 -SiC coating reduces the electrolyte penetration and corrosion of the cathode material.

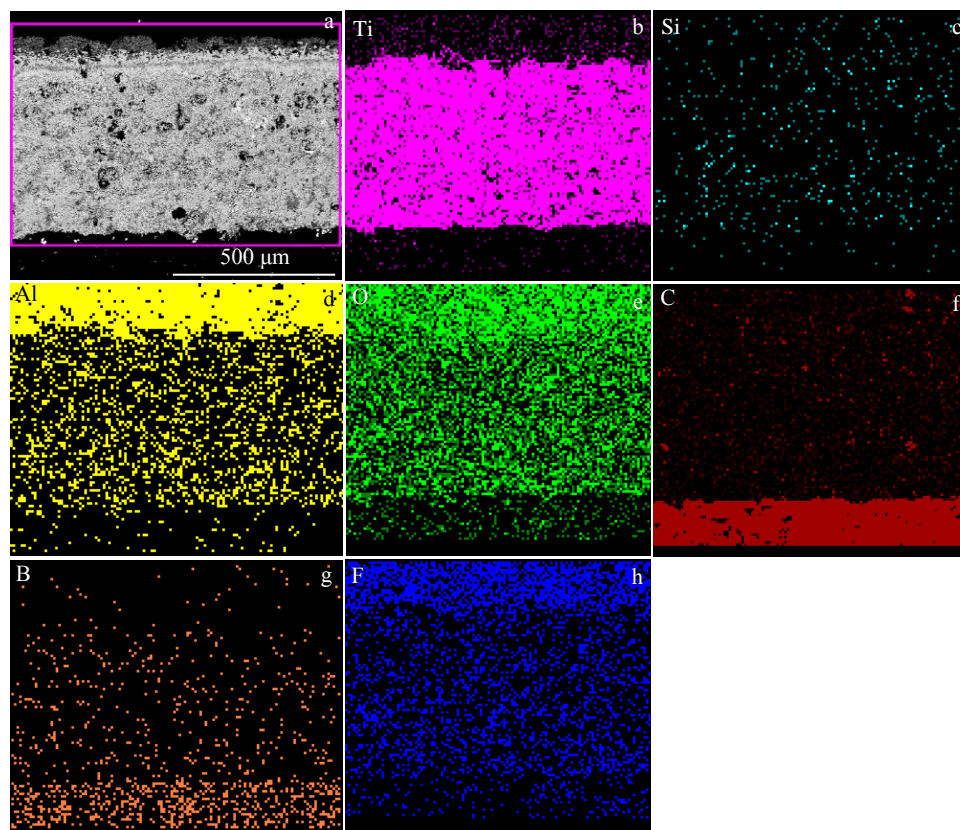


Fig.8 SEM image (a) and element distribution (b-h) of TiB_2 -SiC coating prepared by SAPS after molten salt corrosion

3 Conclusions

1) The TiB₂-SiC coating prepared by SAPS has good oxidation resistance, and there is no obvious ablation at 400 and 800 °C. The oxidation kinetic curves of TiB₂-SiC coating at 400 and 800 °C conform parabolic law. The oxidation rate constants of TiB₂-SiC coating at 400 and 800 °C are $1.92 \times 10^{-5} \text{ mg}^2 \cdot \text{cm}^{-4} \cdot \text{s}^{-1}$ and $1.82 \times 10^{-4} \text{ mg}^2 \cdot \text{cm}^{-4} \cdot \text{s}^{-1}$, respectively.

2) When the temperature is low, the TiB₂-SiC coating is slightly oxidized to form oxidized protective films TiO₂ and B₂O₃ to avoid further oxidation of the coating. When the temperature is high, the formation of dense glassy protective film SiO₂ can seal the pores and cracks generated by oxidation. When the temperature reaches about 1082.4 °C, B₂O₃ evaporates and pores remain inside the coating to increase the contact area of the coating with air, accelerating oxidation of the coating.

3) The TiB₂-SiC coating prepared by SAPS has good resistance to molten salt corrosion. TiB₂-SiC coating maintain a dense structure after molten salt corrosion, and no cracking and peeling of the coating occur. TiB₂-SiC coating has good wettability with aluminum liquid, and forms a tight aluminum liquid barrier layer during electrolysis, which effectively prevents the penetration of molten salt electrolyte into the substrate, and further reduces the penetration and corrosion of electrolyte into the cathode material.

References

- Han X X, Zhang T A, Lv G Z et al. *Journal of the Minerals, Metals & Materials Society*[J], 2019, 71(4): 1574
- Jensen M S, Pezzotta M, Zhang Z L et al. *Journal of the European Ceramic Society*[J], 2008, 16(28): 3155
- Stevens D A. *Journal of Electrochemistry Society*[J], 2001, 148(8): 803
- Zhang X M, Chen W P. *Transactions of Nonferrous Metals Society of China*[J], 2015, 25(6): 1715
- Wang W, Chen W J. *Archives of Metallurgy and Materials*[J], 2019, 64(4): 1257
- Li J, Lv X J, Lai Y Q et al. *Journal of Central South University of Technology*[J], 2008, 15(4): 526
- Koh Y H, Lee S Y, Kim H E. *Journal of the American Ceramic Society*[J], 2001, 84(1): 239
- Xu Z, Fu Q, Lei L et al. *Surface & Coatings Technology*[J], 2013, 226(14): 17
- Zhang Y, Hu H, Ren J et al. *Ceramics International*[J], 2016, 42(16): 18 657
- Yu B, Li H, Han Z et al. *Journal of Thermal Spray Technology* [J], 2013, 22(7): 1201
- Hou X M, Chou K C. *Composites Science and Technology*[J], 2009, 69(16): 2527
- Zhang Y L, Hu Z, Yang B et al. *Ceramics International*[J], 2015, 41(2): 2582
- Zhang Y, Hu Z, Li H et al. *Ceramics International*[J], 2014, 40(9): 14 749
- Joon P, Jong K, Nakazato N et al. *Ceramics International*[J], 2018, 44(14): 17 319
- Zhang Y, Yang B, Zhang P et al. *Ceramics International*[J], 2015, 41(10): 14 579
- Steyer Ph, Mege A, Pech D et al. *Surface and Coatings Technology*[J], 2008, 202(11): 2268
- Wang C, Li K, Huo C et al. *Surface & Coatings Technology*[J], 2018, 348: 81
- Yao X, Li K, Fu Q et al. *Journal of Thermal Spray Technology* [J], 2013, 22(4): 531
- Mohammadi M, Kobayashi A, Javadpour S et al. *Vacuum*[J], 2019, 167: 547
- Dell M B, Gerard, Catalog G O. *Extractive Metallurgy of Aluminum*[M]. New York: Interscience, 1963: 403
- Li Q Y, Li J, Yang J H et al. *Metallurgical & Materials Transactions A*[J], 2007, 38(13): 2358
- Ban Y G. *Thesis for Doctorate*[D]. Shenyang: Northeastern University 2008 (in Chinese)
- Wang Z H, Friis J, Ratvik A P. *Minerals, Metals and Materials Series*[J], 2018, 1321

超音速大气等离子喷涂 TiB₂-SiC 涂层的抗氧化性及耐熔盐腐蚀性能

邹柯^{1,2}, 邓春明², 邹俭鹏¹, 刘敏², 刘学璋², 赵瑞敏³, 李顺华³, 朱仁波¹, 高迪¹

(1. 中南大学粉末冶金国家重点实验室, 湖南长沙 410083)

(2. 广东省新材料研究所现代材料表面工程技术国家工程实验室 广东省现代表面工程技术重点实验室, 广东广州 510650)

(3. 云南云铝涌鑫铝业有限公司, 云南红河 663000)

摘要: 采用超音速大气等离子喷涂制备全包覆 TiB₂-SiC 涂层, 研究了 TiB₂-SiC 涂层在 400 和 800 °C 的氧化性能, 并探究其氧化机理。对 TiB₂-SiC 涂层在 900 °C 下的抗铝熔盐腐蚀性能进行研究, 并探讨其耐熔盐腐蚀机理。结果表明, 超音速大气等离子喷涂制备的 TiB₂-SiC 涂层具有良好的抗氧化性, 在 400 °C 的氧化速率常数为 $1.92 \times 10^{-5} \text{ mg}^2 \cdot \text{cm}^{-4} \cdot \text{s}^{-1}$, 在 800 °C 的氧化速率常数为 $1.82 \times 10^{-4} \text{ mg}^2 \cdot \text{cm}^{-4} \cdot \text{s}^{-1}$ 。超音速大气等离子喷涂制备的 TiB₂-SiC 涂层在 900 °C 下具有良好的抗熔盐腐蚀性能, 熔盐腐蚀后 TiB₂-SiC 涂层都保持致密结构, 未发生涂层的开裂及剥落。

关键词: 超音速大气等离子喷涂; TiB₂-SiC 涂层; 抗氧化性能; 耐熔盐腐蚀性能

作者简介: 邹柯, 女, 1995 年生, 硕士, 中南大学粉末冶金国家重点实验室, 湖南长沙 410083, 电话: 0731-88876630, E-mail: zoujp@csu.edu.cn